Radiocarbon, Vol 00, Nr 00, 2023, p 1–12 DOI:10.1017/RDC.2023.47
Selected Papers from the 24th Radiocarbon and 10th Radiocarbon & Archaeology International Conferences, Zurich, Switzerland, 11–16 Sept. 2022

CENTENNIAL TO MILLENNIAL-SCALE FLUCTUATIONS OF THE LAKE SUIGETSU ATMOSPHERIC ^{14}C RECORD REPRESENT AUTHENTIC ^{14}C FEATURES OVER LAST GLACIAL-TO-DEGLACIAL TIMES

Michael Sarnthein[1]* • Pieter M Grootes[2] • Manfred Mudelsee[3]

[1]Institute of Geosciences, University of Kiel, Olshausenstr. 40, 24098 Kiel, Germany
[2]Institute of Ecosystem Research, University of Kiel, Olshausenstr. 40, 24098 Kiel, Germany
[3]Climate Risk Analysis, Kreuzstrasse 27, Heckenbeck, 37581 Bad Gandersheim, Germany

ABSTRACT. Short-term fluctuations in atmospheric radiocarbon (^{14}C) concentration mark the tree-ring record for the last ~15 kyr. Terrestrial macrofossils from sediment cores of Lake Suigetsu, Japan, extend this record of fluctuations back to >35 cal ka BP. Their significance, however, is under debate since the signal-to-noise ratio of the Suigetsu record is low and progressively decreases with increasing age. Coherent semi-millennial-scale structures of the Suigetsu ^{14}C record have nevertheless been identified by three different techniques, namely visual inspection, analyses of the first derivative of ^{14}C vs. calendar age, and Bayesian spline inflections of ^{14}C concentration vs. calendar age, and hence appear objectively real. These ^{14}C fluctuations correlate closely with those of the tree-ring-based ^{14}C master record ~10–14 cal ka. Thus, Suigetsu fine structures attain global significance and may properly reflect atmospheric ^{14}C variability back to ~35 cal ka. Carbonate-based ^{14}C records from speleothems and ocean sediments are far smoother and form, together with Suigetsu and other data, the backbone of the IntCal20 record >14 cal ka that largely lacks the Suigetsu fine structure. ^{14}C decay reduces ^{14}C-signal amplitudes over time, so Holocene-style ^{14}C signals of solar modulation disappear in the noise beyond ~10 cal ka. The remaining older ^{14}C fine structures had larger forcings, most likely linked to climate and carbon cycle, especially ocean-atmosphere CO_2 exchange, and thus contain valuable information about these factors. They may also provide global stratigraphic tie points to correlate ^{14}C records of oceanic plankton sediments and climate signals independent of problems with local ^{14}C reservoir effects.

KEYWORDS: fluctuations in atmospheric radiocarbon record 10–30 cal ka, fluctuations in tree-ring-based radiocarbon record, origin of pre-Holocene atmospheric radiocarbon fluctuations, Suigetsu atmospheric radiocarbon record.

INTRODUCTION

For the conversion of radiocarbon (^{14}C) ages of last glacial-to-early-deglacial times into calendar age equivalents we are faced with the problem of finding two differently focused, in part intimately interrelated empirical data sets that compare ^{14}C years with paired calendar years as outlined further below.

The IntCal20 calibration curve with its 1σ standard deviation predictive envelope provides the best-possible conversion of atmosphere-related ^{14}C ages to calendar age equivalents back to 55 cal. ka BP that is presently available. Back to ~14 or ~15 cal ka BP, it relies on the tree ring-based "master records" of atmospheric ^{14}C concentration (Reimer et al. 2020). Prior to ~15 cal ka BP and the continuous tree-ring record, IntCal20 uses a Bayesian spline to integrate evidence from a broad mixture of different ^{14}C records (Reimer et al. 2020). On the one hand, the IntCal20 (international consensus) calibration curve thus incorporates atmospheric ^{14}C ages of (short) floating tree-ring records and lacustrine sediment records based on carefully picked plant macrofossils for the record of Lake Suigetsu (Bronk Ramsey et al. 2020).

On the other hand, IntCal20 is strongly controlled by many ^{14}C records of marine sediment piles (hardly laminated), corals, and speleothem sections. Several carbonate-based records have

*Corresponding author. Email: michael.sarnthein@ifg.uni-kiel.de

the great advantage of paired U/Th age control (e.g., those from Hulu Cave; Cheng et al. 2018), but widely suffer from, in part little known, variable short-term ^{14}C offsets either from the coeval atmospheric concentration due to variable marine reservoir ages or from changes in the soil reservoir effect of cave deposits. Those variables are only rarely constrained by multiple precise data series (Wang et al. 2022). The carbonate-based indirect atmospheric ^{14}C records show less fine structure than the Suigetsu record.

Problems to refine and correlate the outlined different time series were overcome by new statistical analyses, using a Bayesian spline procedure that also incorporates calendar age uncertainty and an additive error term on the ^{14}C determinations to provide a statistically robust calibration curve (with uncertainties no greater than on previous iterations). As a result, most fine-scale fluctuations in the relationship between ^{14}C concentration and cal. age estimates are smoothed out and/or treated as "noise" in IntCal20 beyond the range of tree-ring calibration (Reimer et al. 2020).

Prior to ~15 cal ka BP, the Suigetsu ^{14}C record, although a component of IntCal20, forms the only direct and quasi-continuous record of atmospheric ^{14}C concentrations free of any potential inherent variations of reservoir and dead-carbon age back to >35 cal ka BP (a limit chosen for practical use in this paper). Originally optical varve counts of Suigetsu sediment sections had been considered as a valuable tool to generate an independent line of evidence of absolute age control, a great perspective (Schlolaut et al. 2018). This approach was proven false by further independent age information outlined below.

Sections between 17.285 and 40.408 m core depth with weak-and-thin or no lamination resulted in different calendar ages for varve counts by microscopy and µXRF (micro-X-Ray fluorescence) and necessitated a varve interpolation program to derive a time scale down to 40 m (Schlolaut et al. 2018). Sarnthein et al. (2020) tested the two varve timescales using as test case the age of the lower end of ^{14}C plateau no. 2b, the oldest ^{14}C structure and tie point that can be constrained by µXRF-based varve counts (Marshall et al. 2012). In contrast to an age of 16.4 cal ka BP proposed by optical varve counts (Schlolaut et al. 2018), the µXRF-based counts reveal an age of ~16.9 cal ka BP. This value matches directly a third, independent age estimate, the U/Th model-based Suigetsu timescale with an age estimate of 16.94 cal ka BP (Bronk Ramsey et al. 2020). This point-match and the increasing undercount of optical varves with age (Bronk Ramsey et al. 2020; Sarnthein et al. 2020; Figure 3) clearly support the use of the latter ages for the Suigetsu record as "best possible" approximation.

In summary, we followed Bronk Ramsey et al. (2020) and finally replaced the ages based on optical varve counts by the updated U/Th-based model ages deduced from a complex correlation scheme to U/Th-based ages of the Hulu speleothem record (Bronk Ramsey et al. 2020; ages updated by dataset of Cheng et al. 2018).

Different from the widely smoothed IntCal20 curve, the Suigetsu record of atmospheric ^{14}C concentrations ~10 to ~35 cal ka BP appears to display a whole suite of fairly distinct centennial-to-millennial-scale fluctuations. Their quality, authenticity, and origin are the topic of this study that mainly re-evaluates data sets recently published (Bronk Ramsey et al. 2020). If confirmed, these fluctuations, at least the ^{14}C plateau boundaries, will provide a suite of atmospheric, thus global stratigraphic tie points to correlate glacial-to-deglacial records of changes in climate and ocean. In particular, the age tie points provided by these ^{14}C structures will reduce the problem of properly assigning cal. age estimates by interpolation over long ^{14}C plateau periods with varying climate and sedimentation conditions down to the scale of a ^{14}C

https://doi.org/10.1017/RDC.2023.47 Published online by Cambridge University Press

plateau. During LGM and early deglacial times, however, long, largely horizontal scatter bands of approximately constant ^{14}C ages may span up to 1200 yr. Also, the suite of structures *per se* may provide tie points for initial age correlation (Sarnthein et al. 2007, 2020).

THE SUIGETSU ATMOSPHERIC ^{14}C RECORD—DATA BASE

The noisy Suigetsu ^{14}C record is based on an average macrofossil sample density of ~8 to ~20, rarely 35 ^{14}C dates per thousand years (kyr), as compared to a modeled time resolution of 200 ^{14}C ages/cal. kyr for IntCal20 (Reimer et al. 2020). The glacial-to-deglacial Suigetsu record of ^{14}C ages between 14 and 28 cal ka BP (Figure 1) is not a straight slope line but shows a suite of sections with no or little slope, other sections with a rapid decrease in ^{14}C age with decreasing calendar age, labeled "plateaus" and "jump" structures. Comparison with ^{14}C structures displayed by the tree-ring record 10–15 cal ka BP (Figure 3) shows close similarity making the probability that the Suigetsu ^{14}C structures might result from chance deposition low. The significance of these Suigetsu centennial to millennial-scale features beyond the tree ring record and 15 cal ka BP is under debate since their signal-to-noise ratio in the record is low and, in some cases, does not allow rejection of the null hypothesis assuming a straight line for the correlation of ^{14}C and cal age data (Bard and Heaton 2021).

Plateaus extend over ~400 to ~1200 yr each, some being less, some more distinct (Sarnthein et al. 2020), where the lower value of (300 to) 400 yr has been dictated by the ^{14}C sample density of hemipelagic *marine* sediment sections from all over the ocean (in contrast to the much higher sample resolution of the Suigetsu *lacustrine* record discussed here), moreover by the ^{14}C measuring uncertainty in this age range. The question is in which way this apparent centennial-to-millennial-scale structure of the Suigetsu ^{14}C record can be identified objectively and reproducibly. In the ^{14}C age domain the suite of ^{14}C age fluctuations has been defined by visual inspection of "age plateaus" (rules of definition described in the Text Box 1; Sarnthein et al. 2007) giving a result fully congruent with structures based on the first derivative of the ^{14}C age-to-calendar age relationship and its 1σ uncertainty range, obtained by using a running kernel window (Sarnthein et al. 2015).

An independent approach plots the Suigetsu atmospheric ^{14}C record for the period 14–30 cal ka BP as $\Delta^{14}C$ deviations from the standard atmosphere vs. IntCal20 cal age (Figure 2). The curve is here defined by a Bayesian spline (Bronk Ramsey et al. 2020; Bard and Heaton 2021). All in all, periods of gradually decreasing $\Delta^{14}C$ values are reflecting 15 atmospheric ^{14}C age plateaus (blue numbers) and their 1σ-uncertainty range. In between, (rapid) rises in $\Delta^{14}C$ are directly compared with ^{14}C age "jump"' between plateaus. In Figure 2 these inflections in the Bayesian spline directly face the Suigetsu-based plateau and jump structures as derived by visual inspection and by the first derivative of ^{14}C ages in the time domain, here plotted as dark pink line segments in the $\Delta^{14}C$ domain (Supplementary Table 1S). In general, the two presentations agree well especially considering the exaggerated jumps in atmospheric ^{14}C concentration induced by the "simplifying" assumption of an on-average constant Suigetsu ^{14}C age over a "horizontal" ^{14}C scatter band of a plateau-episode. This assumption is needed where insufficient data was available to say, whether very short-term ^{14}C changes within the plateau may be real.

For the period from 27 to 30 cal ka BP, plateaus numbered 10b and 11 deviate from the Bayesian plot. Here the Suigetsu ^{14}C data appear to have a problem since ^{14}C ages, generated by different laboratories, diverge by up to 1000 yr at analytical 1σ uncertainties of ~150 to below 400 yr (Bronk Ramsey et al. 2012). Our plateau definitions tried to bridge the

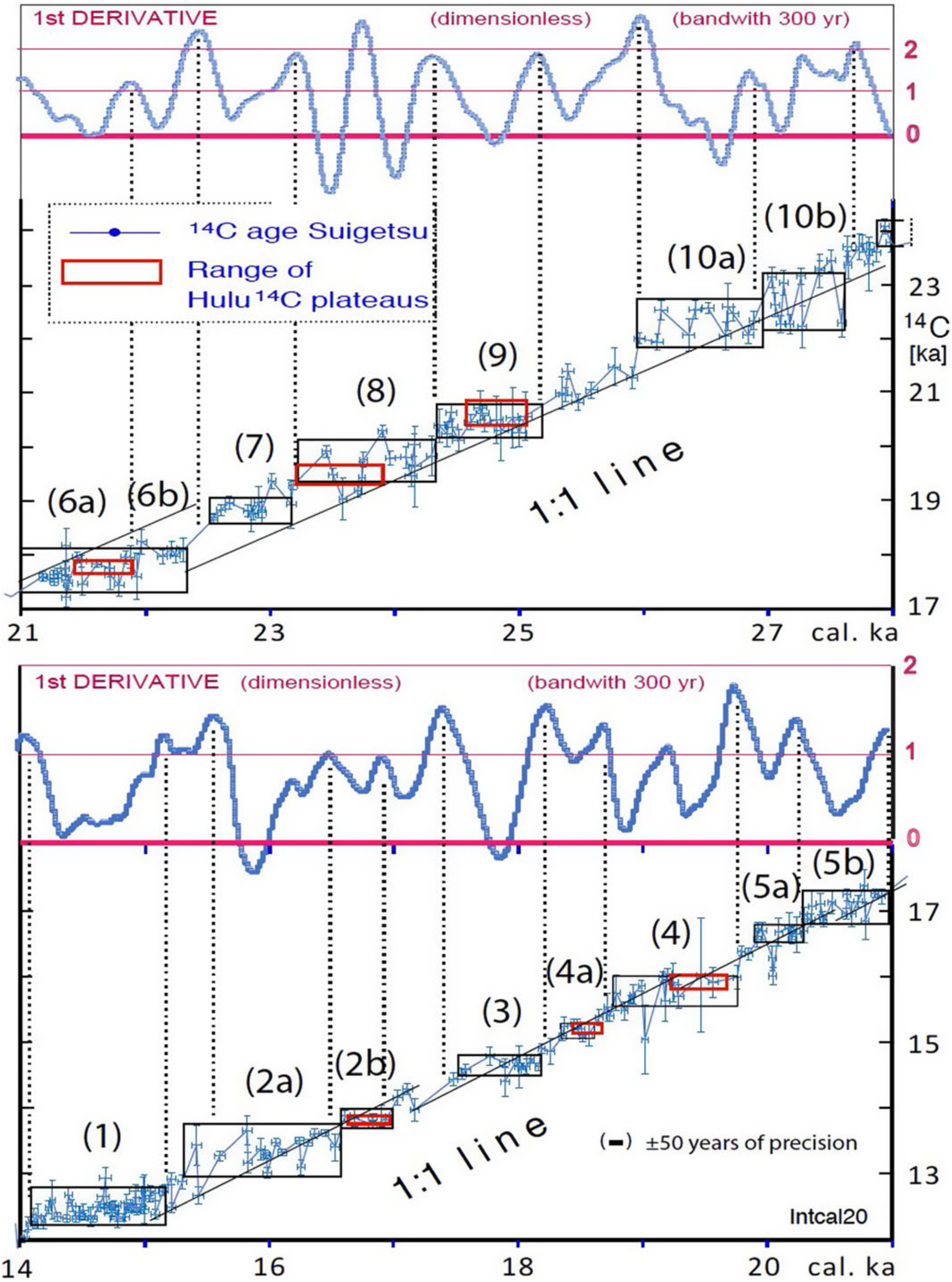

Figure 1 Atmospheric ^{14}C ages and error bars of Lake Suigetsu plant macrofossils vs. U/Th-based model age of 15–21 (bottom) and 21–27 (top) cal ka BP (blue dots; Sarnthein et al. 2020, modified, using age data of Bronk Ramsey et al. 2020). ^{14}C plateaus longer than 400 yr (in case of plateau 4a: 250 yr) are outlined by a suite of labeled horizontal boxes that envelop scatter bands of largely constant or slightly rising ^{14}C ages, separated by "^{14}C jumps," statistically best defined by maximum spikes in the 1st derivative plot and 1σ uncertainty range. For rules of plateau definition see Text Box 1.

https://doi.org/10.1017/RDC.2023.47 Published online by Cambridge University Press

Box 1 Definition of atmospheric ^{14}C plateaus derived from tree rings and the Lake Suigetsu sediment section (following Sarnthein et al. 2007, 2015, 2020).

(1) The term "^{14}C plateau" is assigned to a set of largely constant atmospheric ^{14}C ages over a range extending over 250/400 to 1200 consecutive cal yr. This leads to a horizontal, in part slightly oblique scatter band of atmospheric ^{14}C ages (Figure 1), in the Lake Suigetsu section measured with a time resolution of 8–20, rarely up to 35 ^{14}C data per 1000 yr.

(2) ^{14}C age is assumed constant over the full period of the plateau ("horizontal" plateau) because data resolution is insufficient to define a statistically significant true ^{14}C slope over the plateau period.

(3) The upper and lower margin of the plateau (Y-axis) are chosen such that 90% of the ^{14}C ages are within these boundaries (1.6 σ criterion; in Figure 1 delineated by horizonal lines).

(4) From 10 to 21 cal. ka, the typical scatter/uncertainty range of an average plateau ^{14}C age amounts to ±100–250 ^{14}C yr, at cal ages of >21 cal ka BP, especially >23 cal. ka, the uncertainty range is rising up to ±500 yr due to an increased analytical error.

(5) Most lower and upper cal age boundaries (X-axis) of an atmospheric ^{14}C plateau are identified visually by ^{14}C age jumps, that form tipping points of the ^{14}C curve, where the ^{14}C curve is crossing the horizontal border lines assigned to the upper and lower margins of the plateau's uncertainty range, hence is deviating beyond the scatter band of a ^{14}C plateau.

(6) The rapid change in ^{14}C age over cal. age at plateau boundaries is reflected by a distinct maximum of the 1st-derivative of the curve for the ^{14}C age vs. cal age record. The 1st-derivative thus provides a second, statistical plateau identification.

(7) The cal. age of most atmospheric plateau boundaries, assigned halfway between the two nearest ^{14}C ages, can be constrained with a precision of ±50 to ±70 yr on the basis of Suigetsu ^{14}C ages calibrated by U/Th model ages of Bronk Ramsey (2020).

discrepancy by weighted average values. The Bard and Heaton (2021) Bayesian spline in Figure 2, apparently, treated the discrepancy differently.

Although comparison of Figure 1 and 2 indicates that it is possible to objectively and reproducibly identify a fine structure in the noisy atmospheric ^{14}C Suigetsu record, the question remains whether this fine structure is local or has wider significance. The answer is found in Figure 3 that presents a further important line of evidence for the reasoning discussed in this study: It shows the high-resolution Suigetsu atmospheric record (Bronk Ramsey et al. 2020) (Figure 3, right Y-axis) together with the highly detailed tree-ring-based ^{14}C master record (Reimer et al. 2020; Adolphi et al. 2017) (Figure 3, left Y-axis). Atmospheric ^{14}C-age jumps and plateaus between ~10 and ~15 cal ka BP have been defined by scatter bands of largely constant ^{14}C ages extending over >400 yr each. Based on visual inspection most Suigetsu structures agree with the analogous, largely coeval ^{14}C-age structures of the tree-ring-based master record of atmospheric ^{14}C ages. The fit largely applies to the length of the various plateaus, in some cases also to internal plateau structures. This finding suggests that the clearly paired Suigetsu-based centennial-to-millennial-scale fluctuations in ^{14}C concentration for the period 10 to ~15 cal ka BP are indeed real and reflect a global atmospheric ^{14}C signal.

DISCUSSION

In a next step, we tried to corroborate the authenticity of Suigetsu atmospheric ^{14}C structures by testing our visual match of Suigetsu- and tree ring-/floating tree ring-based ^{14}C structures

https://doi.org/10.1017/RDC.2023.47 Published online by Cambridge University Press

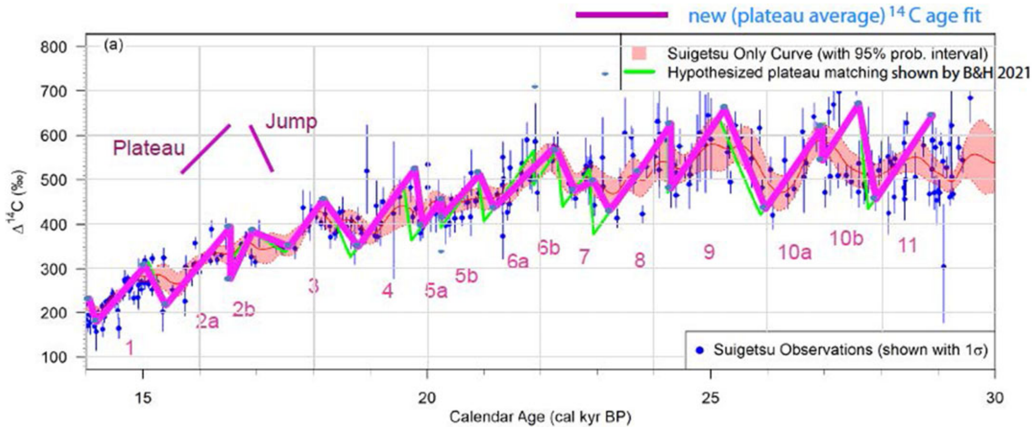

Figure 2 Raw ^{14}C data of Lake Suigetsu (blue dots), converted into the deviation of atmospheric ^{14}C concentration from the (modern) standard atmosphere (in ‰ $\Delta^{14}C$ units), plotted vs. cal. ages of Bronk Ramsey et al. (2020). A Bayesian spline named "Suigetsu only curve" (pink band) (Bard and Heaton 2021, Figure 3a modified) shows periods of gradually decreasing atmospheric $\Delta^{14}C$ values, reflecting 15 atmospheric ^{14}C age plateaus and their uncertainty range as defined and listed by Sarnthein et al. (2020; Table 1). In between, rapidly increasing atmospheric $\Delta^{14}C$ values reflect short gaps and/or ^{14}C age "jumps" between plateaus. Periods where gradually decreasing $\Delta^{14}C$ values balance out the rate of ^{14}C decay provide the horizontal age plateaus, as outlined in the Discussion section. Superimposed are straight line segments in green (Bard and Heaton 2021, called "B&H 2021") and dark pink (modified from Sarnthein et al. 2020; using the revised ages of Bronk Ramsey et al. 2020) that display the atmospheric $\Delta^{14}C$ structures as defined both by visual inspection of raw ^{14}C ages and the 1st derivative technique (Figure 1; Sarnthein et al. 2015). Based on a careful check of the position of plateau boundaries (rules of definition in Text Box 1), we slightly revised three of them previously published (Sarnthein et al. 2020): (i) a slight upward shift of the base of plateau 7, (ii) omission of the boundary between plateaus 6b and 6a, and (iii) a minimal backward shift of the 5a-b plateau boundary by a single age date.

from ~10 to ~15 cal ka BP by means of statistical methods, that is, by calculating the "binned correlation coefficients" (Mudelsee 2014: Section 7.5.1 therein) for both time series (Figures 3 and 4a, b). Indeed, the visual match is well supported by these quantitative analyses of the association between the two time least-squares regression and used to derive short-term trend residuals and binned correlation coefficients both for ^{14}C records, shown in Figure 4 and Supplement Figure S1.

The "binned correlation coefficient" is the same as the ordinary Pearson's correlation coefficient, however, calculated on the respective averages within time bins of the two time series. The very existence of persistence or "memory" in a time series (which is typical for climate) on a particular grid of time values allows us to infer the correlation with other time series that are observed on a different grid. From the estimated persistence times and the average temporal spacings, we determined an optimal bin width of 100 years (Mudelsee 2014: Eq. 7.48 therein). The calculated binned correlation coefficient between the Suigetsu- and the tree-ring-based values then equals 0.90 with a 95% calibrated Student's *t* confidence interval of [0.86; 0.93], which means a significant correlation that is very high. Thus, the visual match is well supported by these quantitative analyses of the association between the two time series.

Thus, the paired tree ring-based master record of annual changes in atmospheric ^{14}C concentration provides conclusive evidence that the suite of semi-millennial features of Suigetsu provides insights into a kind of authentic feature of ^{14}C records that was intrinsic for late deglacial times, a feature with global significance.

https://doi.org/10.1017/RDC.2023.47 Published online by Cambridge University Press

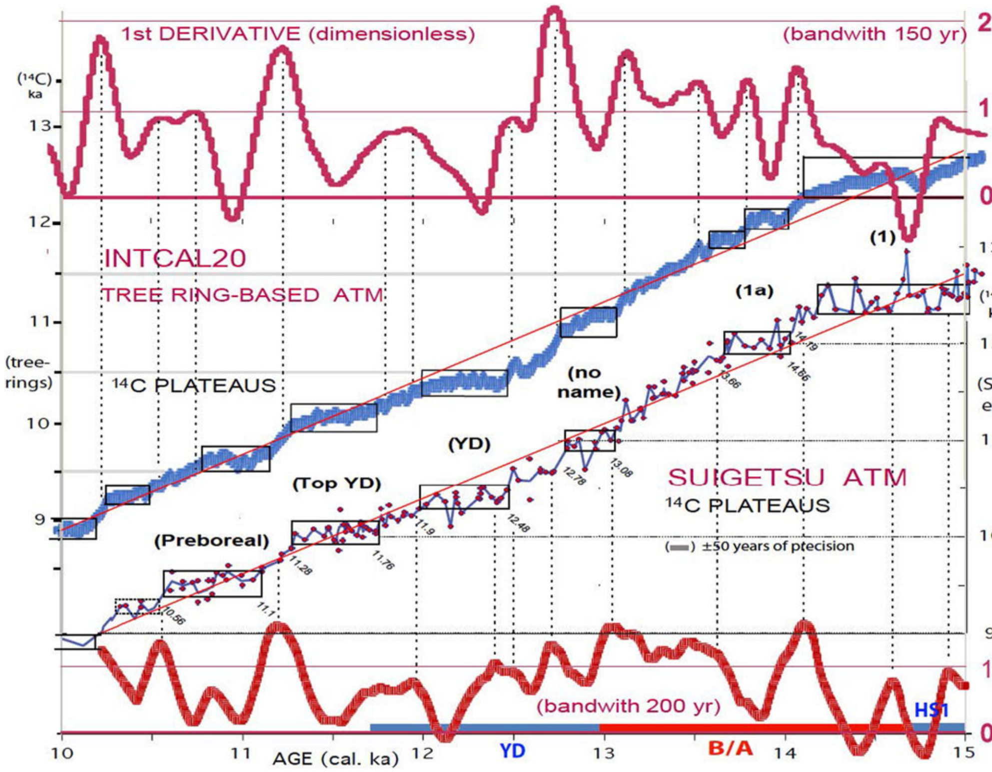

Figure 3 High-resolution record of atmospheric ^{14}C age jumps and plateaus (i.e., a suite of labeled horizontal boxes that envelop scatter bands of largely constant ^{14}C ages extending over >400 cal. yr; for definition of plateaus see Text Box 1) in a sediment section of Lake Suigetsu (Figure 2 of Sarnthein et al. 2020) vs. tree ring-based ^{14}C age jumps and plateaus 10–15 cal ka BP (Reimer et al. 2020; 14.0–14.8 cal. ka BP: suppl. by data of Adolphi et al. 2017). Also, ^{14}C age jumps and most plateau boundaries are highlighted by maximums in the 1st derivative record of ^{14}C per cal years and 1σ uncertainty range (bandwith of 150 yr for tree-ring record; 200 yr for Suigetsu record). Blue line averages paired double and triple ^{14}C ages of Suigetsu plant macrofossils. Age control points (black, at plateau boundaries, in cal. ka) follow varve counts (Schlolaut et al. 2018) incorporated by U/Th model-based ages of Bronk Ramsey et al. (2012, 2020) on the 2020-time scale. YD = Younger Dryas, B/A = Bølling-Allerød (after Steffenson et al. 2008). Red lines depict long-term trend of tree ring- and Suigetsu-based ^{14}C ages 10–15 cal ka BP each. The perfectly overlapping trendlines (joint slope of 0.78 ± 0.03 and intercepts of 1009 ± 364 yr for Suigetsu vs. 992 ± 415 yr for tree ring record) are derived from linear ordinary least-squares regression and used to derive short-term trend residuals and binned correlation coefficients both for ^{14}C records, shown in Figure 4 and Supplement Figure S1.

Necessarily, the significance of the centennial to millennial structure of the Suigetsu atmospheric ^{14}C record may be extrapolated to the preceding early deglacial and peak glacial time span 15–30 cal ka BP, when major tree ring records are widely absent for further confirmation and ^{14}C records without much fine structure from carbonate archives have largely dominated the IntCal20 record. Accordingly, Suigetsu terrestrial macrofossils extend—without break—the actual atmospheric ^{14}C record beyond the range of tree rings from ~15 cal ka BP back to >~35 cal ka BP. The latest results on ^{14}C variability in floating tree-ring sections older than 14 cal ka BP, presented at the 24th Radiocarbon Conference in Zürich (Friedrich et al. 2022), largely agree with the Suigetsu atmospheric ^{14}C record.

From 20 to 35 cal ka BP, the global significance of the plateau and jump structures in the Suigetsu ^{14}C record is supported by the fact that a large portion of these structures can also be

https://doi.org/10.1017/RDC.2023.47 Published online by Cambridge University Press

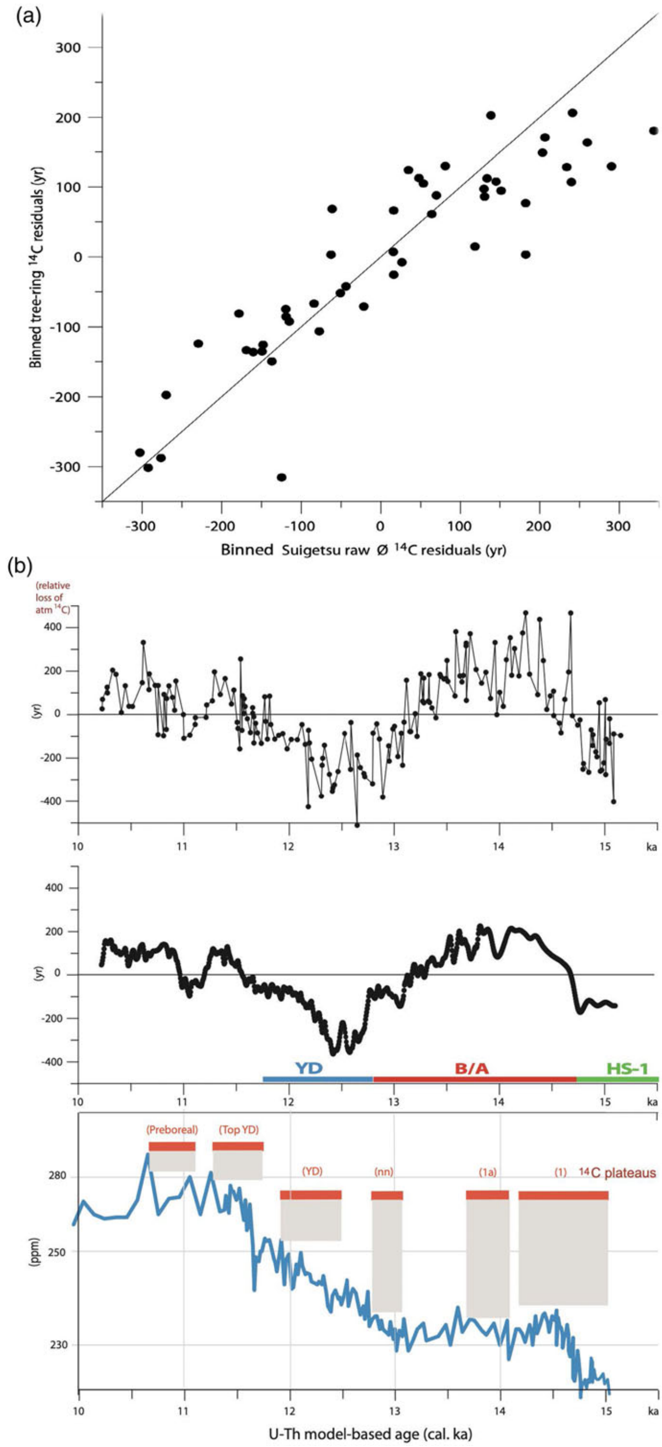

Figure 4 Binned correlation coefficient for the atmospheric ^{14}C records of Lake Suigetsu and tree-ring-based ^{14}C record of IntCal20 (Bronk Ramsey et al. 2020; Reimer et al. 2020; methods of binned correlation in Mudelsee 2014). (a) Binned correlation coefficient of Suigetsu- vs. tree-ring-based trend residuals, assuming a bin width of 100 yr. Correlation coefficient is $r = 0.90$ with 95% confidence interval (0.85; 0.93). (b) Trend residuals (plus zero lines) of Suigetsu- and tree ring-based ^{14}C ages 10–15 cal ka BP (shown in Figure S1) are compared to the cal. age range of the Younger Dryas (YD), Bølling-Allerød (BA), and Heinrich-1 stadial (HS-1) (following Steffensen et al. 2008), the position and extent of atmospheric ^{14}C plateaus (*sensu* Sarnthein et al. 2020), and the late deglacial rise in atmospheric pCO_2 at 15–10 cal ka BP (West Antarctic CO_2 record of Marcott et al. 2014), showing that ^{14}C plateaus are clearly related to a coeval rise in pCO_2.

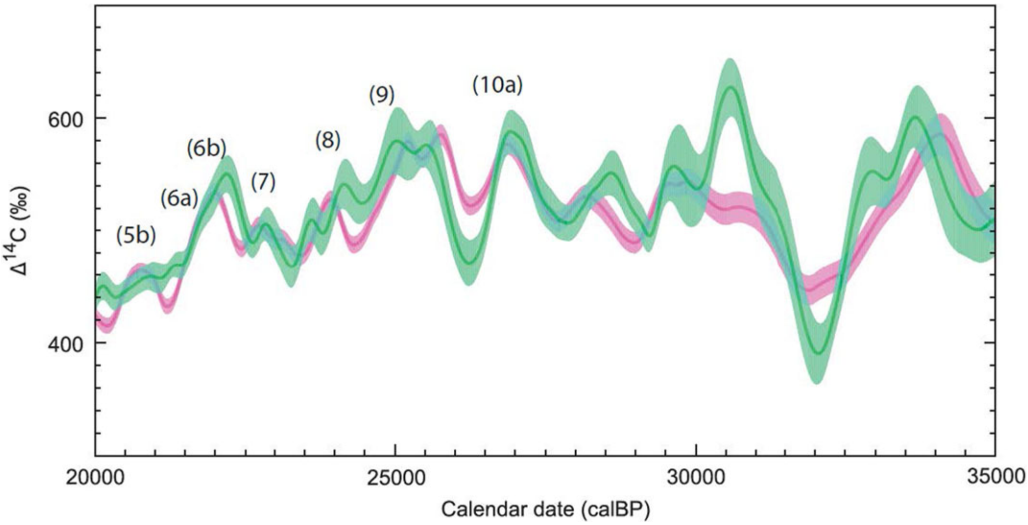

Figure 5 A comparison of Bayesian spline compilations of datasets of Suigetsu (green) and Hulu speleothem, transformed using a MatLab deconvolution algorithm (linear ramp with mean of 420 yr) (magenta) over the period 20–35 cal. ka. Gradually decreasing atmospheric $\Delta^{14}C$ values reflect atmospheric ^{14}C age plateaus and their uncertainty range (black numbers in brackets). Rising $\Delta^{14}C$ values reflect atmospheric ^{14}C age jumps. (Courtesy of Bronk Ramsey et al. 2020.)

seen in a Bayesian spline of analogous $\Delta^{14}C$-based structures in the independent deconvoluted U/Th-dated ^{14}C record derived from Hulu Cave data (Figure 5; Bronk Ramsey et al. 2020). The Hulu Cave record was admittedly smoothed and is generally interpreted as being subject to a ~460 yr dead-carbon reservoir effect with limited variability. In fact, however, the Hulu speleothem may have (also) been affected by allegedly constant, but fairly unknown variations of the local "reservoir effect of soil organic carbon" in the Hulu speleothem over the time span under discussion (Southon et al. 2012; Noronha et al. 2015; Cheng et al. 2018; Reimer et al. 2020). In view of the joint U/Th basis of age control for both the ^{14}C records of Suigetsu und Hulu Cave (as presented by Bronk Ramsey et al. 2020), various distinct centennial-scale offsets of some Hulu Cave ^{14}C features from those of Suigetsu (such as near to 22, 24, 26, and 28.5 cal ka BP) perhaps may reflect short-lasting shifts in the soil-carbon fraction of the Hulu record, now treated as a constant dead carbon fraction of 460 yr (Southon et al. 2012).

Our conclusions on the authenticity of atmospheric ^{14}C-age structures have important implications for global age correlation of marine and terrestrial sediment records records that concern (i) their dating, (ii) quantification of local differences in ^{14}C concentration, and (iii) information on carbon cycle and climate interactions. As detailed in Sarnthein et al. (2020), both visual inspection and spikes of the 1st derivative of the Suigetsu atmospheric ^{14}C record (Figure 1), that are sharp in marking episodes of rapid change, suggest that the cal. ages of the upper and lower plateau boundaries may serve as global age tie points for the age correlation of marine sediment records. The robustness and uncertainty of these structures are best age-calibrated by the data of Bronk Ramsey et al. (2020) at the marked ^{14}C-age jumps that separate two subsequent ^{14}C plateaus each, the range of which is marked by enveloping "boxes" in the Suigetsu record of Figures 1 and 3. Accordingly, the uncertainty of cal. age estimates of the beginning and/or end of an atmospheric ^{14}C plateau hardly exceeds ~50 to ~100 years each, when employing the trends of age estimates listed by Bronk Ramsey et al. (2020). ^{14}C plateau identification in marine sediment records requires a largely constant marine reservoir age

https://doi.org/10.1017/RDC.2023.47 Published online by Cambridge University Press

(MRA) over the total length of a plateau. Otherwise, the atmospheric ^{14}C plateaus would not be reflected as a plateau in ocean surface plankton. Also, the average ^{14}C age of any tree-ring- and/or Suigetsu-based ^{14}C plateau may be compared to that of any coeval plateau properly identified in ocean sediment archives. The difference in ^{14}C average age estimated for paired, that is, for coeval atmospheric and marine plateaus will serve as robust estimate of local marine reservoir ages.

Finally, a major question concerns the potential origin of the centennial-to-millennial-scale fluctuations of atmospheric ^{14}C concentration found at Suigetsu, the only purely atmospheric record without any assumptions on secondary effects. ^{14}C decay reduces the original ^{14}C-signal amplitude over time so, different from the Holocene, clear ^{14}C signals of solar modulation with peak-to-peak values of ~3 pMC (percentage Modern Carbon) necessarily disappear below the 2σ level of detection sensitivity in deglacial-to-glacial records. As a result, most of the ^{14}C structure visible beyond 8–10 cal ka BP originally was connected to larger signals and, most likely, to changes in climate and the ocean-atmosphere CO_2 exchange (first suggested by Stuiver and Braziunas 1993, on the basis of residual $\Delta^{14}C$ of the Holocene long-term trend).

The latter hypothesis receives independent support by distinct structures, that is, from two pronounced negative millennial-scale excursions in the record of ^{14}C-age residuals at 15.2–14.4 and 13.2–11.7 cal. ka (Figure 4b top and Figure S1). They represent a negative deviation of actual ^{14}C ages from the long-term detrended ^{14}C-age records 10-15 cal ka BP for the tree ring- and Suigetsu-based ^{14}C records each. The subsequent rise in ^{14}C-age residuals parallels the very end (and subsequent interstadial) of a pronounced cold climate spell such as the Younger (YD) (12.8–11.7 cal ka BP) and the final phase of Heinrich Stadial 1 (HS1) (~15.1–14.6 cal ka BP). A third increase in ^{14}C-age residuals, a distinct fast rise in ^{14}C age, follows a minor negative excursion of ^{14}C trend residuals, that is centered near 11 cal ka BP and goes along with the Preboreal cold spell.

Near the end of cold stadials, the positive excursion of ^{14}C-age residuals, that is, a relatively fast increase in ^{14}C ages and reduced deviation from the long-term average in years (Figure S1) reflects *per se* a transient dilution of atmospheric ^{14}C by "old" oceanic CO_2 (Figure 4b bottom). In particular, this drop in ^{14}C has paralleled a major ^{14}C plateau and/or cluster of ^{14}C plateaus named "YD" and "1". Most likely, they were linked to short-term deglacial events of enhanced release of "old" CO_2 from the (deep) ocean to the atmosphere reaching 12–13 ppm each (Figure 4b bottom) (Marcott et al. 2014). The CO_2 release may reflect a major change, in part a reversal in ocean Meridional Overturning Circulation (Sarnthein et al. 1994, 2013; Bauska et al. 2021; Yu et al. 2022). If the causal relationships deduced for Figure 4b are extrapolated to earlier times, that is, to the early deglacial and peak glacial ^{14}C record, they may suggest a series of events marked by a short-term ocean-driven rise in atmospheric CO_2 and corresponding transient, gradually fading out reduction in atmospheric ^{14}C unrecorded till now. Altogether, these processes may form a mechanism suitable to explain the origin of the suite of ^{14}C plateaus characteristic of the Suigetsu ^{14}C record (Figures 1, 2, and 5) (Yu et al. 2022; cf. Vettoretti et al. 2022).

In summary, the Suigetsu ^{14}C fine structure may contain valuable information on past interactions between climate change, ocean-atmosphere CO_2 exchange and the carbon cycle beyond 15 cal. ka during deglacial and peak glacial times. These centennial-to-millennial-scale signals can also be traced in high-resolution ^{14}C records of (hemipelagic) ocean plankton sediments (Sarnthein et al. 2020).

CONCLUSIONS AND IMPLICATIONS

Detailed evaluation and tests of the Suigetsu atmospheric ^{14}C record suggest the following results:

- The centennial-to-millennial-scale features in the noisy Suigetsu ^{14}C record can be objectively identified. Such structures in the Suigetsu atmospheric ^{14}C record can be identified by three different techniques, namely visual inspection, first derivative, and Bayesian spline inflections, the results of which largely agree.
- The atmospheric ^{14}C features of the Suigetsu record are authentic and have global significance because on the basis of "binned correlation coefficients" the fine structures of both the highly detailed global IntCal20 tree ring and the noisier Suigetsu ^{14}C record ~10–15 cal ka BP are closely coherent.
- Suigetsu ^{14}C ages extend beyond the reach of tree-ring dates ~15 cal ka BP, without break, the record of atmospheric ^{14}C oscillations back to >35 cal. ka BP. Between 20 and 35 cal ka BP, they are widely reproduced by structures depicted in the carbonate-based and U/Th dated ^{14}C record of the Hulu speleothem, though the oscillations may have been smoothed.
- Most likely the origin of semi-millennial-scale ^{14}C fluctuations was linked to the global carbon cycle, that is, to changes in global climate, ocean meridional overturning circulation, and ocean-atmosphere CO_2 exchange, since ^{14}C decay has too strongly attenuated the potential forcing of solar modulation of ^{14}C signals prior to the Holocene.

Once precisely age-calibrated, the suite of features and age tie points in the atmospheric Suigetsu ^{14}C record have major implications, providing a potential tool and corner stone for the global stratigraphic correlation of analogous ^{14}C records deduced from shallow-dwelling oceanic plankton in sediment records that follows the ^{14}C-age signals of the atmosphere.

SUPPLEMENTARY MATERIAL

To view supplementary material for this article, please visit https://doi.org/10.1017/RDC.2023.47

ACKNOWLEDGMENTS

We are grateful to Dr. S. Beil, University of Kiel, for generous computer assistance. We particularly appreciate the highly constructive and careful suggestions of a reviewer in two successive reviews. He was exceptionally aware of a robust reasoning important for the general implications of our manuscript, and its linguistically sound wording.

REFERENCES

Adolphi F, Muscheler R, Friedrich M, Güttler D, Wacker L, Talamo S, Kromer B. 2017. Radiocarbon calibration uncertainties during the last deglaciation: insights from new floating tree-ring chronologies. Quaternary Science Reviews 170:98–108.

Bard E, Heaton TJ. 2021. On the tuning of plateaus in atmospheric and oceanic ^{14}C records to derive calendar chronologies of deep-sea cores and records of ^{14}C marine reservoir age changes. Climate of the Past 17:1701–1725. doi: 10.5194/cp-17-1701-2021

Bauska TK, Marcott SA, Brook EJ. 2021. Abrupt changes in the global carbon cycle during the last fgacial period. Nature Geoscience 14:91–96.

Bronk Ramsey C, Staff RA, Bryant CL, Brock F, Kitagawa H, van der Plicht J, Schlolaut G, Marshall MH, Brauer A, Lamb HF, et al. 2012. A complete terrestrial radiocarbon record for 11.2 to 52.8 kyr B.P. Science 338:370–374.

Bronk Ramsey C, Heaton TJ, Schlolaut G, Staff RA, Bryant CL, Lamb HF, Marshall MH, Nakagawa T. 2020. Reanalysis of the atmospheric radiocarbon calibration record from Lake Suigetsu, Japan. Radiocarbon. doi: 10.1017/RDC.2020.18

Cheng H, Edwards RL, Southon J, Matsumoto K, Feinberg JM, Sinha A, Zhou W, Li H, Li X, Xu Y, et al. 2018. Atmospheric $^{14}C/^{12}C$ changes during the last glacial period from Hulu Cave. Science 362:1293–1297.

Friedrich M. 2022. European glacial tree-ring chronologies—new high-resolution ^{14}C series. ^{14}C. 24th Radiocarbon and 10th ^{14}C & Archaeology international Conference. C04-04.

Marcott SA, Bauska TK, Buizert C, Steig EJ, Rosen JL, Cuffey KM, Fudge TJ, Severinghaus JP, Ahn J, Kalk ML, et al. 2014. Centennial-scale changes in the global carbon cycle during the last deglaciation. Nature 514:616–619. doi: 10.1038/nature13799

Marshall, M, Schlolaut, G, Nakagawa, T, Lamb, H, Brauer, A, Staff, R, Bronk Ramsey, C, Tarasov, P, Gotanda, K, Haraguchi, T, Yokohama, Y, Yonenobu, H, Tada, R, Suigetsu 2006 Project members. 2012. A novel approach to varve counting using mXRF and X-radiography in combination with thin-section microscopy, applied to the Late Glacial chronology from Lake Suigetsu, Japan. Quaternary Geochronology 13:70–80.

Mudelsee M. 2014. Climate time series analysis: classical statistical and bootstrap methods. 2nd edition. Springer Ed. Cham, Heidelberg, New York, London. doi: 10.1007/978-3-319-04450-7.

Noronha AL, Johnson KR, Southon JR, Hu C, Ruan J, McCabe-Glynn S. 2015. Radiocarbon evidence for decomposition of aged organic matter in the vadose zone as the main source of speleothem carbon. Quaternary Science Reviews 127:37–47.

Reimer PJ, Austin WEN, Bard E, Bayliss A, Blackwell PG, Ramsey CB, Butzin M, Cheng H, Edwards RL, Friedrich M, et al. 2020. The IntCal20 Northern Hemisphere radiocarbon age calibration curve (0–55 cal kBP). Radiocarbon 62(4):725–757. doi: 10.1017/RDC.2020.41

Sarnthein M, Balmer S, Grootes PM, Mudelsee M. 2015. Planktic and benthic ^{14}C reservoir ages for three ocean basins, calibrated by a suite of ^{14}C plateaus in the glacial-to-deglacial Suigetsu atmospheric ^{14}C record. Radiocarbon 57:129–151.

Sarnthein M, Grootes PM, Kennett JP, Nadeau M. 2007. ^{14}C reservoir ages show deglacial changes in ocean currents and carbon cycle. Geophysical Monograph – American Geophysical Union 173:175–196.

Sarnthein M, Küssner K, Grootes PM, Ausin B, Eglinton T, Muglia J, Muscheler R, Schlolaut G. 2020. Plateaus and jumps in the atmospheric radiocarbon record – potential origin and value as global age markers for glacial-to-deglacial paleoceanography, a synthesis. Climate of the Past 16:2547–2571. doi: 10.5194/cp-16-2547-2020

Sarnthein M, Schneider B, Grootes PM. 2013. Peak glacial ^{14}C ventilation ages suggest major draw-down of carbon into the abyssal ocean. Climate of the Past 9(1):925–965.

Sarnthein M, Winn K, Jung SJ, Duplessy JC, Labeyrie L, Erlenkeuser H, Ganssen G. 1994. Changes in east Atlantic deep-water circulation over the last 30,000 years: eight time slice reconstructions. Paleoceanography 9(2):209–267.

Schlolaut G, Staff RA, Marshall MH, Brauer A, Bronk Ramsey C, Lamb HF, Nakagawa T. 2018. Microfacies analysis of the Lake Suigetsu (Japan) sediments from ~50 to ~10 ka BP and an extended and revised varve based chronology. Quaternary Science Reviews 200:351–366.

Southon J, Noronha AL, Cheng H, Edwards RL, Wang Y. 2012. A high-resolution record of atmospheric ^{14}C based on Hulu Cave speleothem H82. Quaternary Science Reviews 33:32–41.

Steffensen JP, Andersen KK, Bigler M, Clausen HB, Dahl-Jensen D, Fischer H, Goto-Azuma K, Hansson M, Johnsen SJ, Jouzel J, et al. 2008. High-resolution Greenland ice core data show abrupt climate change happens in few years. Science 321:680. doi: 10.1126/science.1157707

Stuiver M, Braziunas TV. 1993. Modeling atmospheric ^{14}C influences and ^{14}C ages of marine samples to 10,000 B.C. Radiocarbon 35:137–189.

Vettoretti G, Ditlevsen P, Jochum M, Rasmussen SO. 2022. Atmospheric CO_2 control of spontaneous millennial-scale ice age climate oscillations. Nature geoscience 15:300–306.

Wang Zh, Zhang F, Cao Y. 2022. Linking sedimentary and speleothem isotope proxy records to improve lacustrine and marine ^{14}C chronologies. Quaternary Science Reviews 282:107444. doi: 10.1016/quascirev2022.107444

Yu J, Oppo DW, Jin Z, et al. 2022. Millennial and centennial CO2 release from the Southern Ocean during the last deglaciation. Nature Geoscience. doi: 10.1038/s4156-022-00910-9